

Magnetoionic Propagation and Polarization in HF Radio: Phenomenology, Simulation, and Receiver Optimization

Christopher W. Stubbs, with Claude Code
January 2026

Abstract

This report provides a comprehensive treatment of magnetoionic wave propagation in the Earth's ionosphere, with particular emphasis on the practical consequences for HF radio reception. We develop the theory of ordinary (O) and extraordinary (X) mode propagation, demonstrate through simulation that differential D-region absorption creates strongly elliptical—often nearly circular—polarization at the receiver during daytime conditions, and show that this effect has profound implications for optimal receiver antenna selection. The key finding is that **left-hand circular polarization (LCP) feeds provide dramatic signal-to-noise advantages for daytime HF reception in the Northern Hemisphere**, with improvements exceeding 60 dB at lower frequencies. We also clarify the distinct mechanisms of HF fading: polarization fading (eliminated by circular polarization receivers) versus multipath fading from ionospheric irregularities (not eliminated). Extensive simulation results for realistic propagation paths are presented, along with observational data from WWV time signal recordings.

Contents

1	Introduction	4
2	Magnetoionic Theory: Fundamentals	4
2.1	The Ionosphere as a Magnetized Plasma	4
2.2	The Appleton-Hartree Equation	5
2.3	O-Mode and X-Mode: The Two Characteristic Waves	5
3	Differential Absorption: The Key Phenomenon	6
3.1	D-Region Absorption	6
3.2	Why X-Mode Absorbs More Than O-Mode	7
3.2.1	The Fundamental Symmetry Breaking: Electron Gyration	7
3.2.2	Quantitative Absorption Difference	7
3.3	Simulation Results: Differential Loss	8
4	Received Polarization State	8
4.1	Equal Amplitudes: Linear Polarization	8
4.2	Unequal Amplitudes: Elliptical Polarization	9
4.3	Ellipticity Angle and Axial Ratio	9

5 Angular Splitting: Elevation and Azimuth	10
5.1 Elevation Splitting	10
5.2 Azimuth Splitting	10
5.3 Implications for Direction Finding	11
6 Faraday Rotation	11
6.1 Physical Mechanism	11
6.2 Magnitude of Faraday Rotation	12
6.3 Faraday Rotation is NOT the Same as Ellipticity	12
7 Fading Mechanisms in HF Propagation	12
7.1 Polarization Fading (Faraday Fading)	12
7.2 Multipath Fading from Ionospheric Irregularities	13
7.3 Multi-Hop Interference	13
7.4 Absorption Fading	13
7.5 Summary: What Circular Polarization Does and Does Not Fix	13
7.6 An Interesting Consequence: Reduced Fading at Low Frequencies	13
7.7 Polarization Diversity: Exploiting O/X Path Differences	14
7.7.1 O/X Path Separation	14
7.7.2 Ionospheric Irregularity Scales	14
7.7.3 Expected Decorrelation	14
7.7.4 Diversity Gain	15
7.7.5 Implications for Receiver Design	15
7.7.6 Experimental Verification	15
8 Optimal Receiver Polarization: The Critical Choice	15
8.1 The Symmetry Breaking	15
8.2 Quantitative Advantage of Correct Handedness	16
8.3 Night vs Day: When Does It Matter?	16
8.4 Practical Recommendations	17
9 Simulation Results: Detailed Examples	17
9.1 CHU to OVRO (3621 km, 2-hop)	17
9.1.1 Daytime Results (19:00 UTC)	18
9.1.2 Nighttime Results (06:00 UTC)	18
9.2 WWV to Boston (2816 km, 2-hop)	18
9.2.1 Daytime Results	19
10 Three-Dimensional Ray Visualization	20
11 Observational Evidence	21
11.1 CHU Triplet Recordings	21
11.1.1 Daytime Observations (2026-01-07, 13:13 UTC)	21
11.1.2 Nighttime Observations (2026-01-07, 00:44 UTC)	22
11.2 Phase Stability: Evidence for Ionospheric Multipath	23
11.3 Cross-Frequency Correlation	24
11.4 Comparison with Simulation Predictions	24

12 Implications and Applications	25
12.1 Time and Frequency Standards	25
12.2 Amateur Radio	25
12.3 Direction Finding	25
12.4 Ionospheric Research	25
12.5 Useful HF Beacon Stations	26
12.5.1 WWV (Fort Collins, Colorado, USA)	26
12.5.2 WWVH (Kauai, Hawaii, USA)	26
12.5.3 CHU (Ottawa, Canada)	26
12.5.4 RWM (Moscow, Russia)	27
12.5.5 Frequency Coverage Summary	27
12.5.6 Practical Considerations for Ionospheric Research	27
13 Conclusions	27
A Simulation Code	28
B Stokes Parameter Definitions	29

1 Introduction

High-frequency (HF) radio propagation via ionospheric reflection is a complex phenomenon that has been studied for over a century. While the basic principles of ionospheric reflection are well understood, the detailed polarization behavior of HF signals is often overlooked in practical applications. This oversight can result in substantial signal losses—sometimes exceeding 60 dB—that could be avoided with proper antenna selection.

This report addresses several key questions:

1. Why do HF signals arrive with elliptical (often nearly circular) polarization?
2. What determines the handedness (LCP vs RCP) of the dominant polarization?
3. How does this vary with frequency, time of day, and path geometry?
4. What are the implications for receiver antenna design?
5. What causes fading in HF signals, and which types can be mitigated?

The answers to these questions have significant practical implications for:

- Time and frequency standard reception (WWV, CHU, etc.)
- Amateur radio operations
- Over-the-horizon radar
- HF direction finding
- Ionospheric research

2 Magnetoionic Theory: Fundamentals

2.1 The Ionosphere as a Magnetized Plasma

The ionosphere is a weakly ionized plasma permeated by the Earth's magnetic field. This combination creates a *birefringent* medium—one in which the propagation characteristics depend on the polarization state of the wave.

Key parameters characterizing the magnetoionic medium:

$$f_p = \frac{1}{2\pi} \sqrt{\frac{N_e e^2}{\epsilon_0 m_e}} \approx 9\sqrt{N_e} \text{ Hz} \quad (\text{plasma frequency}) \quad (1)$$

$$f_H = \frac{eB}{2\pi m_e} \approx 1.4 \text{ MHz} \quad (\text{electron gyrofrequency}) \quad (2)$$

$$X = \left(\frac{f_p}{f} \right)^2 \quad (\text{normalized plasma parameter}) \quad (3)$$

$$Y = \frac{f_H}{f} \quad (\text{normalized magnetic parameter}) \quad (4)$$

where N_e is electron density (m^{-3}), B is magnetic field strength (T), and f is wave frequency.

2.2 The Appleton-Hartree Equation

The refractive index n of the ionosphere is given by the Appleton-Hartree equation:

$$n^2 = 1 - \frac{X}{1 - iZ - \frac{Y_T^2}{2(1-X-iZ)} \pm \sqrt{\frac{Y_T^4}{4(1-X-iZ)^2} + Y_L^2}} \quad (5)$$

where:

- $Y_L = Y \cos \theta$ (longitudinal component, along ray direction)
- $Y_T = Y \sin \theta$ (transverse component, perpendicular to ray)
- θ = angle between wave vector and magnetic field
- $Z = \nu/\omega$ (collision frequency term, causes absorption)
- ν = electron-neutral collision frequency (s^{-1}); in the D-region (60–90 km), $\nu \approx 10^6\text{--}10^7 s^{-1}$ due to high neutral density

The \pm sign gives rise to **two distinct propagation modes**.

2.3 O-Mode and X-Mode: The Two Characteristic Waves

The two solutions to the Appleton-Hartree equation correspond to:

O-mode (Ordinary) The “+” solution. Characterized by:

- Refractive index closer to unity ($n_O \approx 1$)
- Reflects at higher altitude (penetrates deeper into ionosphere)
- Corresponds to **Left-Hand Circular Polarization (LCP)** in Northern Hemisphere
- Lower D-region absorption

X-mode (Extraordinary) The “−” solution. Characterized by:

- Refractive index deviates more from unity
- Reflects at lower altitude
- Corresponds to **Right-Hand Circular Polarization (RCP)** in Northern Hemisphere
- Higher D-region absorption

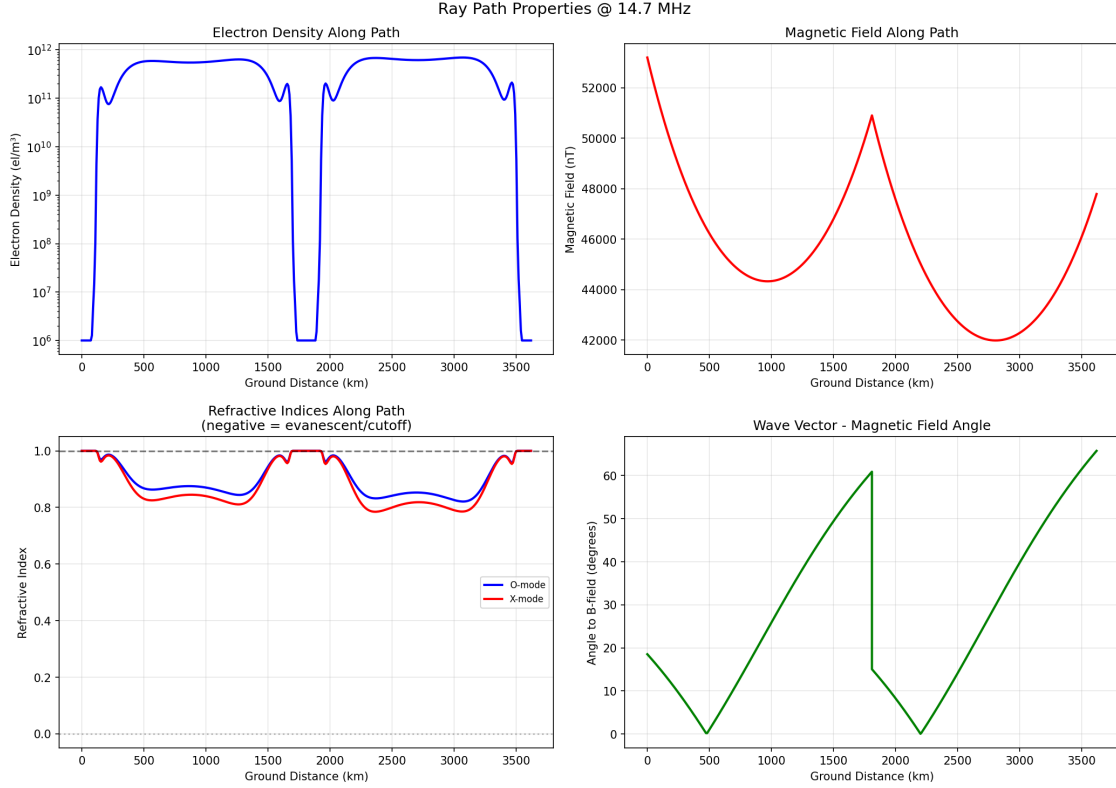


Figure 1: Refractive indices along a daytime CHU-to-OVRO path. The O-mode (blue) maintains $n \approx 1$ longer, penetrating deeper before reflecting. The X-mode (red) reflects at lower altitude. The difference in path length contributes to (but is not the dominant cause of) differential loss.

3 Differential Absorption: The Key Phenomenon

3.1 D-Region Absorption

The D-region (60–90 km altitude) is characterized by:

- Relatively high collision frequency $\nu \approx 10^6\text{--}10^7 \text{ s}^{-1}$ (i.e., 1–10 MHz equivalent)
- Moderate electron density $N_e \approx 10^8\text{--}10^9 \text{ m}^{-3}$ (exists only during daytime)
- Significant wave absorption, especially at lower frequencies

The high collision frequency arises from the relatively dense neutral atmosphere at these altitudes. Electrons oscillating in the wave field collide frequently with neutrals, converting wave energy to heat.

The absorption coefficient scales approximately as:

$$\kappa \propto \frac{N_e \nu}{(f^2 + \nu^2)} \quad (6)$$

For typical HF frequencies ($f \gg \nu$), this simplifies to $\kappa \propto N_e \nu / f^2$, giving the characteristic f^{-2} frequency dependence of ionospheric absorption.

3.2 Why X-Mode Absorbs More Than O-Mode

3.2.1 The Fundamental Symmetry Breaking: Electron Gyration

The key to understanding differential absorption lies in the motion of electrons in a magnetic field. Due to the Lorentz force ($\mathbf{F} = q\mathbf{v} \times \mathbf{B}$), electrons spiral around magnetic field lines with a specific handedness: when viewed along the magnetic field direction, electrons gyrate in a **right-handed** sense (clockwise when B points toward the observer).

This gyration has a characteristic frequency—the electron gyrofrequency $f_H \approx 1.4$ MHz. The handedness of electron motion breaks the symmetry between left and right circular polarizations:

- **X-mode (RCP in Northern Hemisphere):** The wave's electric field rotates in the *same* sense as the electron gyration. This allows resonant coupling—the electrons can continuously absorb energy from the wave as they spiral. Result: **enhanced absorption**.
- **O-mode (LCP in Northern Hemisphere):** The wave's electric field rotates *opposite* to the electron gyration. The electrons cannot maintain phase with the driving field. Result: **reduced absorption**.

This is analogous to pushing a child on a swing: pushing in phase with the natural motion (X-mode) transfers energy efficiently, while pushing out of phase (O-mode) does not.

3.2.2 Quantitative Absorption Difference

The critical insight is that O and X modes have **different absorption coefficients**. For frequencies well above the gyrofrequency ($f \gg f_H \approx 1.4$ MHz), the non-deviative absorption scales approximately as:

$$\kappa_O \propto \frac{1}{(f + f_H)^2} \cdot (\text{base absorption}) \quad (7)$$

$$\kappa_X \propto \frac{1}{(f - f_H)^2} \cdot (\text{base absorption}) \quad (8)$$

Since the X-mode denominator is smaller (for $f > f_H$), X-mode absorption is always higher than O-mode. The ratio of absorption coefficients is:

$$\frac{\kappa_X}{\kappa_O} = \left(\frac{f + f_H}{f - f_H} \right)^2 \quad (9)$$

At 5 MHz: $\kappa_X/\kappa_O \approx 3.2$ (X-mode absorbs 220% more)

At 10 MHz: $\kappa_X/\kappa_O \approx 1.8$ (X-mode absorbs 80% more)

At 15 MHz: $\kappa_X/\kappa_O \approx 1.5$ (X-mode absorbs 50% more)

For typical conditions, X-mode experiences 50–200% higher absorption than O-mode per unit path length, with the effect strongest at lower frequencies. For paths with:

- Multiple hops (more D-region traversals)
- Lower frequencies (higher base absorption)
- Daytime conditions (D-region present)

The cumulative effect can be **enormous**—differential losses exceeding 60 dB are possible.

3.3 Simulation Results: Differential Loss

Table 1 shows simulated differential absorption for two representative paths.

Table 1: Differential O/X absorption for daytime paths (19:00 UTC)

Path	Freq (MHz)	Loss _O (dB)	Loss _X (dB)	ΔLoss (dB)	LCP/RCP ratio	LCP/RCP (dB)
<i>CHU to OVRO (3621 km, 2-hop)</i>						
	3.33	339	404	65	>1000	>60
	7.85	177	182	5.4	3.5	+5.4
	14.67	145	147	1.7	1.5	+1.7
<i>WWV to Boston (2816 km, 2-hop)</i>						
	2.5	426	584	158	>1000	>100
	5.0	232	246	14	26	+14
	10.0	157	160	3.4	2.2	+3.4

Key observation: At 2.5 MHz on the WWV-Boston daytime path, X-mode experiences 158 dB more loss than O-mode. An RCP receiver would see essentially *no signal* while an LCP receiver captures the full O-mode power.

4 Received Polarization State

4.1 Equal Amplitudes: Linear Polarization

When O and X modes arrive with equal amplitudes, the received signal is **always linearly polarized**, regardless of the phase difference between modes.

For equal-amplitude LCP and RCP with phase difference δ :

$$E_x = A\sqrt{2} \cos(\delta/2)e^{i\Phi} \quad (10)$$

$$E_y = A\sqrt{2} \sin(\delta/2)e^{i\Phi} \quad (11)$$

Both components have the *same phase* Φ , so the polarization is linear at angle $\theta = \delta/2$.

Stokes parameters for equal amplitudes:

$$I = 1 \quad (12)$$

$$Q = \cos \delta \quad (13)$$

$$U = \sin \delta \quad (14)$$

$$V = 0 \quad (\text{always zero}) \quad (15)$$

The phase difference (Faraday rotation) only *rotates* the linear polarization; it does not create ellipticity.

4.2 Unequal Amplitudes: Elliptical Polarization

When differential absorption makes $A_O \neq A_X$, the polarization becomes elliptical:

$$I = A_O^2 + A_X^2 \quad (16)$$

$$Q = 2A_O A_X \cos \delta \quad (17)$$

$$U = 2A_O A_X \sin \delta \quad (18)$$

$$V = A_X^2 - A_O^2 \quad (\text{non-zero!}) \quad (19)$$

The Stokes V parameter indicates circular polarization:

- $V < 0$: Net LCP (O-mode dominates, typical for daytime Northern Hemisphere)
- $V > 0$: Net RCP (X-mode dominates, rare)
- $V = 0$: Linear polarization (equal amplitudes)

4.3 Ellipticity Angle and Axial Ratio

The ellipticity angle χ is defined by:

$$\sin(2\chi) = \frac{V}{I} \quad (20)$$

Range: $-45^\circ \leq \chi \leq +45^\circ$

- $\chi = 0^\circ$: Linear polarization
- $\chi = -45^\circ$: Pure LCP
- $\chi = +45^\circ$: Pure RCP

The axial ratio (minor/major axis) is:

$$\text{AR} = |\tan \chi| \quad (21)$$

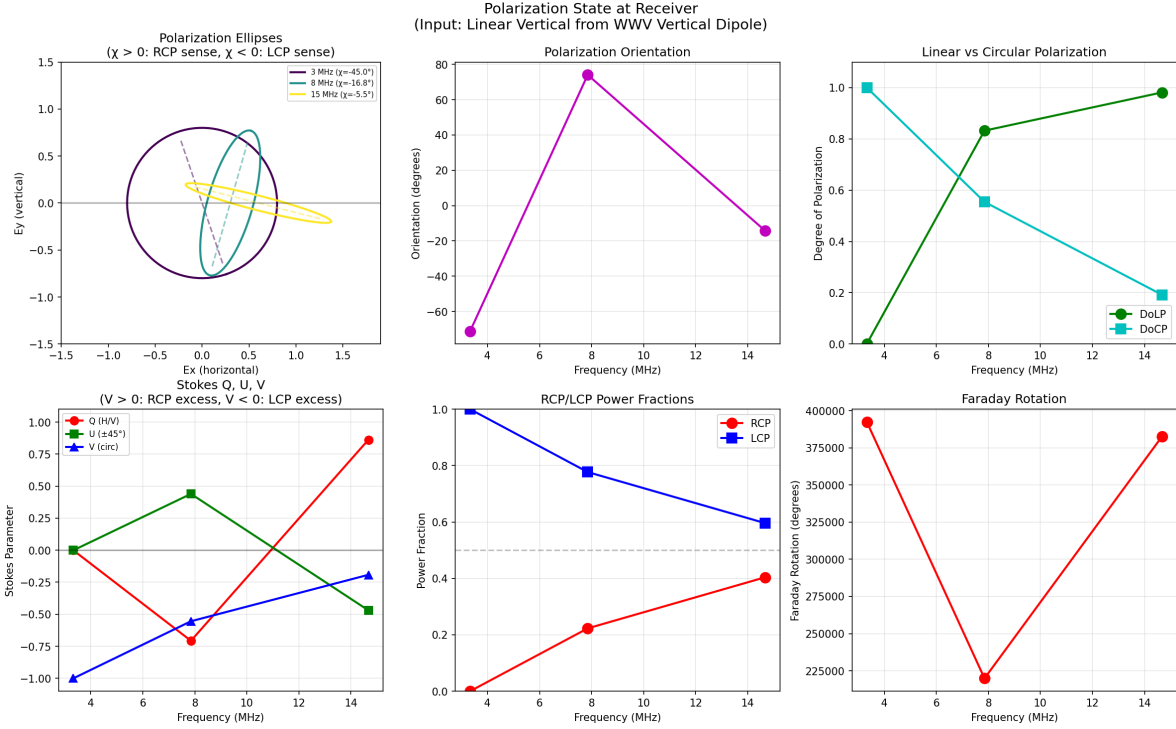


Figure 2: Received polarization state for CHU-to-OVRO daytime path. At 3.33 MHz, the polarization is nearly pure LCP ($\chi \approx -45^\circ$) due to strong X-mode absorption. Higher frequencies show progressively more linear polarization as differential absorption decreases.

5 Angular Splitting: Elevation and Azimuth

5.1 Elevation Splitting

Because O-mode penetrates higher before reflecting, O and X modes arrive at different elevation angles:

- O-mode: Higher elevation angle (longer path, reflects at higher altitude)
- X-mode: Lower elevation angle (shorter path, reflects at lower altitude)

Typical elevation splitting: 0.3–3° depending on frequency and path geometry.

5.2 Azimuth Splitting

The magnetized ionosphere also causes lateral deflection perpendicular to both:

- The electron density gradient (vertical)
- The magnetic field direction

This creates azimuthal (lateral) splitting between O and X modes, typically 0.1–1° for mid-latitude paths.

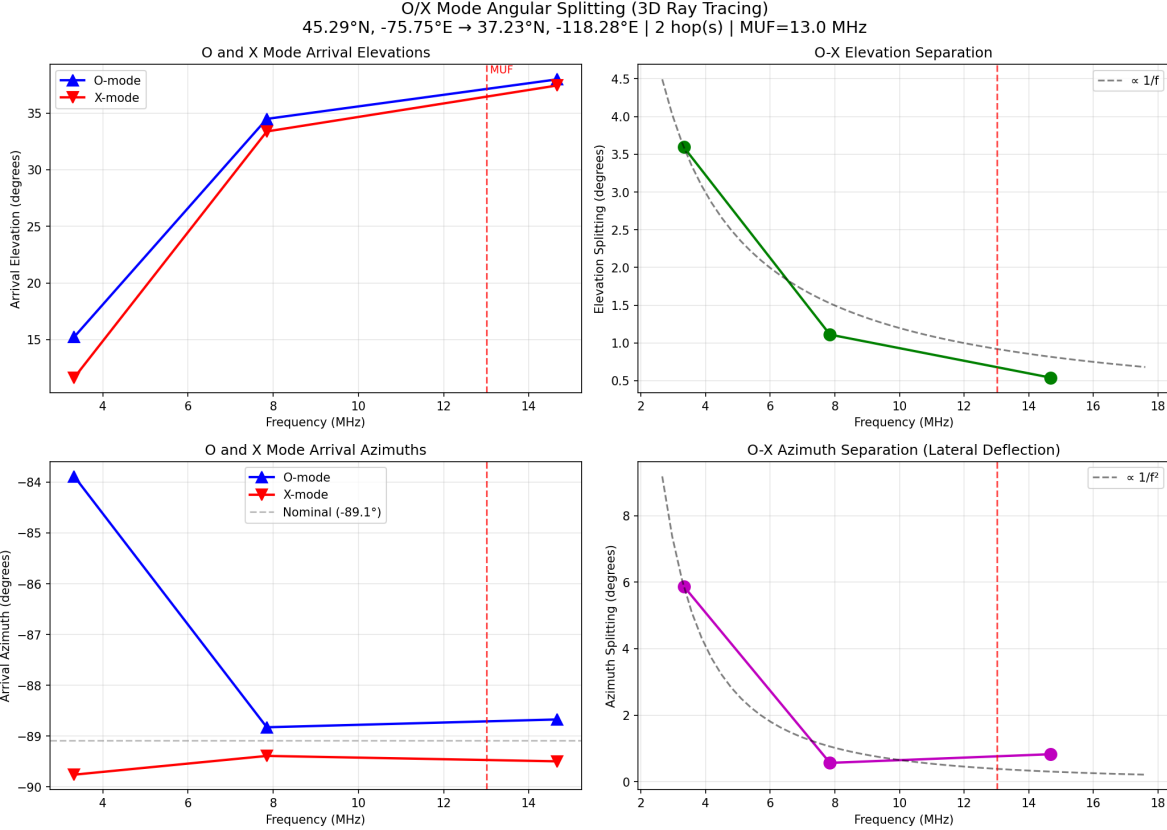


Figure 3: O/X angular splitting for CHU-to-OVRO daytime path. Upper panels show absolute arrival angles; lower panels show the splitting between modes. The red dashed line indicates the MUF.

5.3 Implications for Direction Finding

The angular splitting has important implications:

- DF systems using linear polarization see a “blurred” source
- Circular polarization feeds can isolate individual modes for cleaner bearings
- The splitting is frequency-dependent, complicating wideband DF

6 Faraday Rotation

6.1 Physical Mechanism

As O and X modes propagate with different phase velocities, they accumulate a phase difference:

$$\delta = \phi_O - \phi_X = 2\Omega \quad (22)$$

where the Faraday rotation angle is:

$$\Omega = \frac{2.365 \times 10^4}{f^2} \int N_e B_{\parallel} ds \quad (\text{radians}) \quad (23)$$

6.2 Magnitude of Faraday Rotation

For typical HF paths:

- $\Omega \propto f^{-2}$ (strong frequency dependence)
- At 5 MHz: Thousands to millions of radians
- At 25 MHz: Hundreds to thousands of radians

The effective polarization angle $\theta = \Omega \bmod 180^\circ$ appears essentially random and varies rapidly with small ionospheric changes.

6.3 Faraday Rotation is NOT the Same as Ellipticity

A common misconception: Faraday rotation does **not** create ellipticity.

- Faraday rotation: Changes the *orientation* of linear polarization
- Differential absorption: Changes the *ellipticity* (creates $V \neq 0$)

Both effects occur simultaneously, but they are physically distinct.

7 Fading Mechanisms in HF Propagation

Understanding fading is crucial for system design. There are several distinct mechanisms:

7.1 Polarization Fading (Faraday Fading)

Mechanism:

1. Linear transmitter launches equal O and X modes
2. Modes accumulate different phases (Faraday rotation)
3. At receiver, they recombine into linear polarization at angle θ
4. Ionospheric variations cause θ to change
5. Linear receiver sees amplitude $\propto \cos(\theta - \theta_{\text{ant}})$
6. Deep fades occur when polarization rotates through antenna null

Mitigation: Eliminated by circular polarization receiver.

A pure LCP or RCP receiver is insensitive to polarization rotation because:

- It receives only one circular component
- The amplitude of a circular component is constant regardless of the linear polarization angle of the combined wave (when both circular components are present)

7.2 Multipath Fading from Ionospheric Irregularities

Mechanism:

1. The ionosphere is not a smooth mirror—it has “crinkles,” traveling ionospheric disturbances (TIDs), and small-scale irregularities
2. A nominally single-hop path actually consists of *many* closely-spaced ray paths
3. These rays have slightly different path lengths (100s of meters to kilometers)
4. At the receiver, they interfere constructively and destructively
5. As the ionosphere evolves, relative phases change → amplitude fading

Key point: This multipath fading affects **both** circular polarizations equally. It is **NOT** eliminated by **circular polarization receivers**.

This is the dominant source of fading observed with circular polarization antennas.

7.3 Multi-Hop Interference

Mechanism:

1. Different hop modes (1F, 2F, 1E, etc.) can arrive simultaneously
2. They have different path lengths → different phases
3. Interference creates fading as relative phases change

Mitigation: Usually one hop mode dominates because path losses differ by 10–30 dB per hop. This is typically a secondary effect.

7.4 Absorption Fading

Mechanism:

1. D-region absorption varies with solar illumination, X-rays, etc.
2. Signal strength varies as absorption changes

Mitigation: Affects both polarizations equally; cannot be mitigated by antenna selection.

7.5 Summary: What Circular Polarization Does and Does Not Fix

Table 2: Fading mechanisms and circular polarization effectiveness

Fading Mechanism	Single CP Fix?	Dual CP (LCP+RCP)
Polarization (Faraday)	Yes	Eliminated
Multipath (irregularities)	No	Diversity gain (see §6.6)
Multi-hop interference	Partial	Mode selection
Absorption variation	No	No

7.6 An Interesting Consequence: Reduced Fading at Low Frequencies

At low frequencies during daytime, when X-mode is almost completely absorbed:

1. The received signal is nearly pure LCP (O-mode only)
2. There is no X-mode to interfere with
3. **Polarization fading cannot occur** because there's only one mode
4. A linear antenna sees constant amplitude from the circular wave

This is counterintuitive: the “worst” propagation conditions (high absorption) actually *reduce* one type of fading by eliminating the mode interference that causes it.

7.7 Polarization Diversity: Exploiting O/X Path Differences

An important question arises for conditions where LCP and RCP powers are comparable (nighttime, or higher frequencies during daytime): *Is the multipath fading correlated between O and X modes?* If not, dual-polarization receivers could exploit polarization diversity for fading mitigation even when differential absorption is negligible.

7.7.1 O/X Path Separation

The O and X modes follow geometrically distinct paths through the ionosphere:

- **Vertical separation:** O-mode reflects 10–30 km higher than X-mode (frequency dependent)
- **Lateral separation:** Azimuth splitting of 0.1–1° corresponds to ~1–10 km at the reflection point
- **Total 3D separation:** Typically 15–40 km between O and X reflection regions

7.7.2 Ionospheric Irregularity Scales

The multipath fading from ionospheric “crinkles” arises from irregularities with characteristic scales:

Table 3: Ionospheric irregularity scales and O/X correlation

Irregularity Type	Horizontal Scale	Vertical Scale	O/X Correlation
Small-scale (scintillation)	0.1–1 km	1–10 km	Uncorrelated
Medium-scale TIDs	10–100 km	10–50 km	Partially correlated
Large-scale TIDs	100–1000 km	50–100 km	Correlated

7.7.3 Expected Decorrelation

For irregularities with correlation lengths comparable to or smaller than the O/X path separation (15–40 km), the fading experienced by each mode samples *different* realizations of the ionospheric structure. This leads to:

- **Small-scale fading:** Essentially uncorrelated between O and X modes
- **Medium-scale fading:** Partially decorrelated (correlation coefficient $\rho \sim 0.3\text{--}0.7$)
- **Large-scale fading:** Correlated ($\rho \sim 0.8\text{--}1.0$)

The dominant contribution to rapid fading (timescales of seconds to minutes) comes from small and medium-scale irregularities, suggesting **significant decorrelation** between O and X mode fading.

7.7.4 Diversity Gain

For a dual-polarization receiver using selection or maximal-ratio combining:

$$\text{Diversity Gain} = 10 \log_{10} \left(\frac{\text{SNR}_{\text{combined}}}{\text{SNR}_{\text{single}}} \right) \quad (24)$$

With uncorrelated Rayleigh fading on two branches, theoretical diversity gain is ~ 10 dB at the 1% outage level. For partially correlated fading ($\rho \sim 0.5$), the gain is reduced but still significant ($\sim 5\text{--}7$ dB).

7.7.5 Implications for Receiver Design

This analysis suggests that dual-polarization (LCP + RCP) receivers provide benefits in *all* conditions:

Table 4: Benefits of dual-polarization reception

Condition	Primary Benefit	Mechanism
Daytime, low freq	SNR improvement	Select stronger mode (LCP)
Daytime, high freq	Moderate SNR + diversity	Mode selection + partial decorrelation
Nighttime	Diversity gain	Uncorrelated multipath fading

7.7.6 Experimental Verification

This prediction is testable with simultaneous LCP/RCP recordings. The key measurement would be the cross-correlation coefficient between LCP and RCP amplitude time series:

$$\rho_{LR}(\tau) = \frac{\langle A_L(t)A_R(t+\tau) \rangle - \langle A_L \rangle \langle A_R \rangle}{\sigma_L \sigma_R} \quad (25)$$

If $\rho_{LR}(0) < 0.7$, significant diversity gain is achievable. The triplet frequency data shows low cross-frequency correlation ($r < 0.1$), suggesting the ionosphere has structure on scales that would also decorrelate O/X paths—but direct LCP/RCP measurements are needed to confirm.

8 Optimal Receiver Polarization: The Critical Choice

8.1 The Symmetry Breaking

The Earth's magnetic field breaks the symmetry between LCP and RCP:

- In the **Northern Hemisphere**: O-mode \rightarrow LCP, X-mode \rightarrow RCP
- In the **Southern Hemisphere**: O-mode \rightarrow RCP, X-mode \rightarrow LCP

Since O-mode always has lower D-region absorption:

- **Northern Hemisphere**: Use LCP receiver for daytime
- **Southern Hemisphere**: Use RCP receiver for daytime

8.2 Quantitative Advantage of Correct Handedness

Table 5 shows the SNR advantage of choosing the correct circular polarization for daytime reception.

Table 5: SNR advantage of LCP over RCP for daytime Northern Hemisphere paths

Path	Freq (MHz)	LCP/RCP (dB)	χ (deg)	Recommendation
CHU-OVRO	3.33	+65	-45	LCP essential
CHU-OVRO	7.85	+5.4	-17	LCP preferred
CHU-OVRO	14.67	+1.7	-5.5	LCP slight advantage
WWV-Boston	2.5	>100	-45	LCP essential
WWV-Boston	5.0	+14	-34	LCP strongly preferred
WWV-Boston	10.0	+3.4	-11	LCP preferred

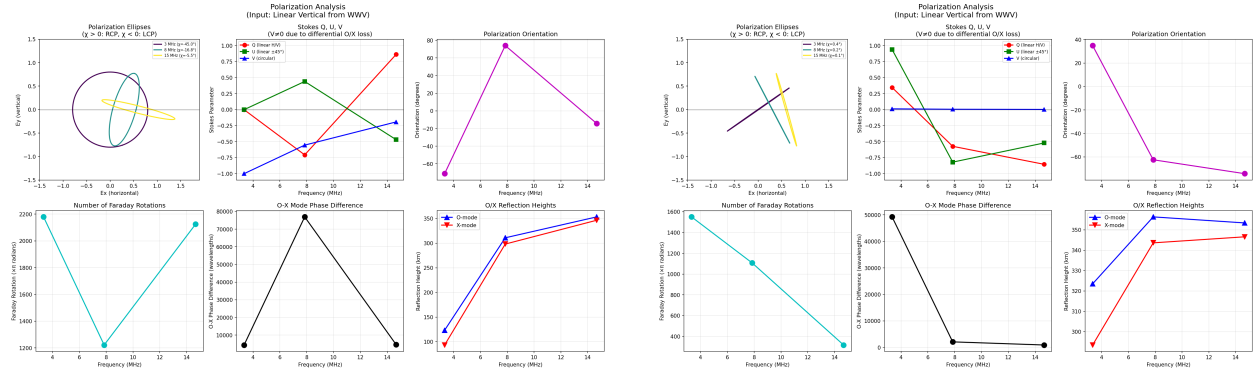
Critical insight: At lower frequencies during daytime, choosing the wrong handedness can mean the difference between a usable signal and no signal at all.

8.3 Night vs Day: When Does It Matter?

At night, the D-region largely disappears:

- Differential absorption becomes negligible
- Received polarization is nearly linear ($V \approx 0$)
- LCP and RCP receive equal power
- Handedness choice doesn't matter for SNR

The advantage of correct circular polarization is primarily a **daytime phenomenon**.



(a) Daytime: Strong ellipticity at low frequencies

(b) Nighttime: Nearly linear polarization

Figure 4: Comparison of received polarization for CHU-to-OVRO path. During daytime (left), low frequencies show strong LCP dominance. At night (right), all frequencies show nearly linear polarization.

8.4 Practical Recommendations

1. **For daytime HF reception in Northern Hemisphere:** Use LCP antenna
2. **For daytime HF reception in Southern Hemisphere:** Use RCP antenna
3. **For nighttime reception:** Either handedness works; linear is also acceptable
4. **For 24-hour operation:** LCP/RCP switchable system, or accept daytime penalty with linear
5. **For low frequencies (<5 MHz) daytime:** Circular polarization is *essential*, not optional

9 Simulation Results: Detailed Examples

9.1 CHU to OVRO (3621 km, 2-hop)

This path from the Canadian time station CHU (Ottawa, 45.29°N , 75.75°W) to the Owens Valley Radio Observatory (37.23°N , 118.28°W) is an excellent test case for demonstrating magnetoionic effects.

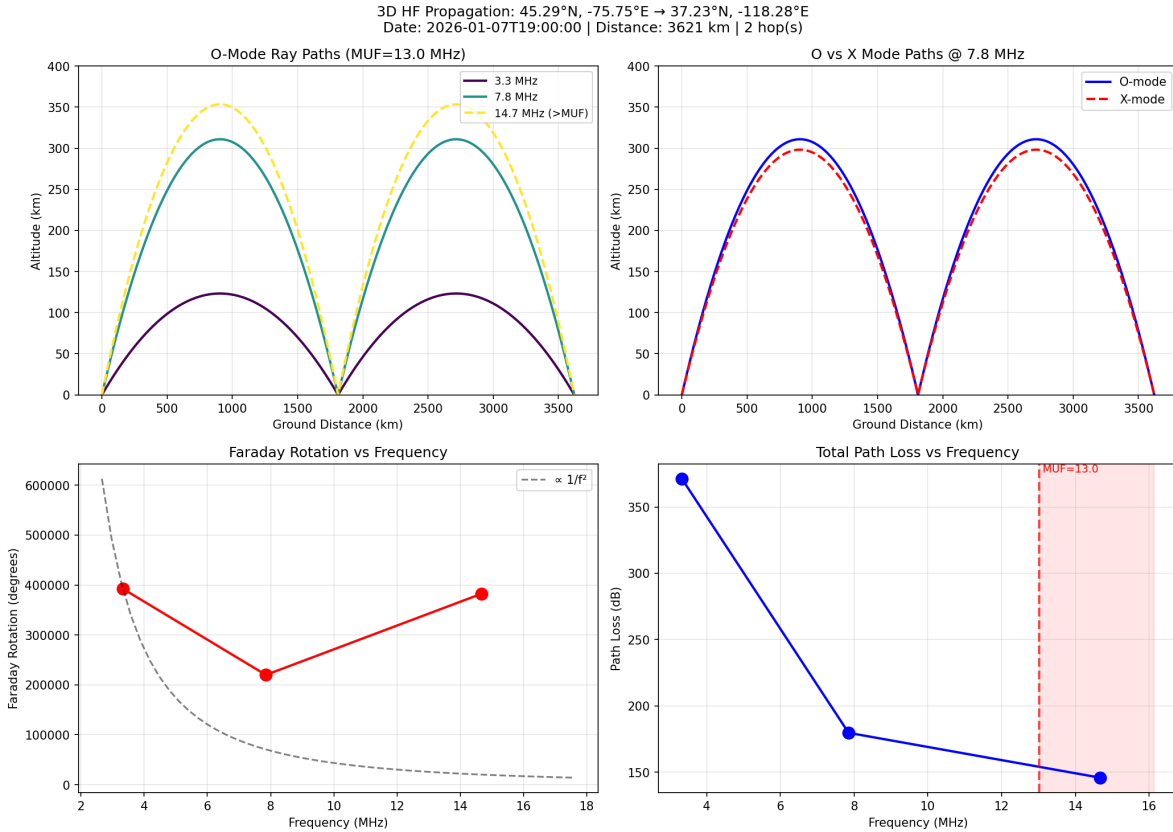


Figure 5: Overview of CHU-to-OVRO daytime propagation. Upper left: Ray paths showing O-mode penetrating higher. Upper right: O vs X comparison. Lower panels: Faraday rotation and path loss vs frequency.

9.1.1 Daytime Results (19:00 UTC)

RECEIVED POLARIZATION (due to differential O/X absorption)

Freq (MHz)	Loss_O (dB)	Loss_X (dB)	DLoss (dB)	LCP/RCP ratio	Ellip (deg)	%LCP	%RCP
3.33	338.7	403.9	65.2	>1000	-45.0	100.0	0.0
7.85	176.9	182.4	5.4	3.49	-16.8	77.7	22.3
14.67	145.0	146.7	1.7	1.48	-5.5	59.6	40.4

At 3.33 MHz, the X-mode is effectively completely absorbed. Only O-mode (LCP) survives.

9.1.2 Nighttime Results (06:00 UTC)

RECEIVED POLARIZATION (due to differential O/X absorption)

Freq (MHz)	Loss_O (dB)	Loss_X (dB)	DLoss (dB)	LCP/RCP ratio	Ellip (deg)	%LCP	%RCP
3.33	114.8	114.7	-0.1	0.98	0.4	49.4	50.6
7.85	122.4	122.4	-0.0	0.99	0.2	49.7	50.3
14.67	127.8	127.8	-0.0	0.99	0.1	49.8	50.2

At night, both modes arrive with equal amplitude—linear polarization.

9.2 WWV to Boston (2816 km, 2-hop)

This east-west path from WWV (Fort Collins, CO) to Boston, MA demonstrates even more dramatic differential absorption due to the longer path through the sunlit D-region.

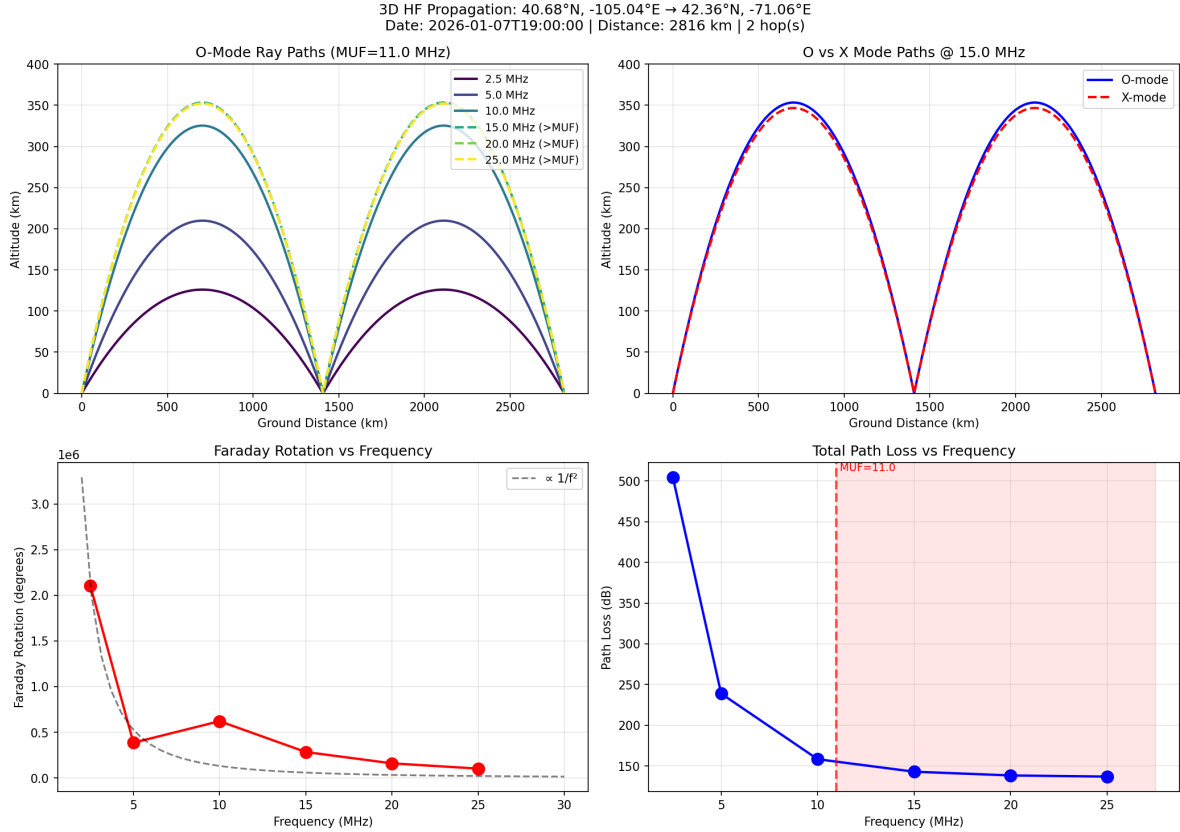


Figure 6: Overview of WWV-to-Boston daytime propagation.

9.2.1 Daytime Results

RECEIVED POLARIZATION (due to differential O/X absorption)

Freq (MHz)	Loss_0 (dB)	Loss_X (dB)	DLoss (dB)	LCP/RCP ratio	Ellip (deg)	%LCP	%RCP
2.50	425.6	583.5	157.9	>1000	-45.0	100.0	0.0
5.00	231.9	246.0	14.1	25.75	-33.9	96.3	3.7
10.00	156.6	160.0	3.4	2.16	-10.8	68.4	31.6
15.00	142.1	143.7	1.6	1.43	-5.1	58.9	41.1

At 2.5 MHz, the differential loss exceeds **150 dB**. This is an extreme case demonstrating why circular polarization selection is critical.

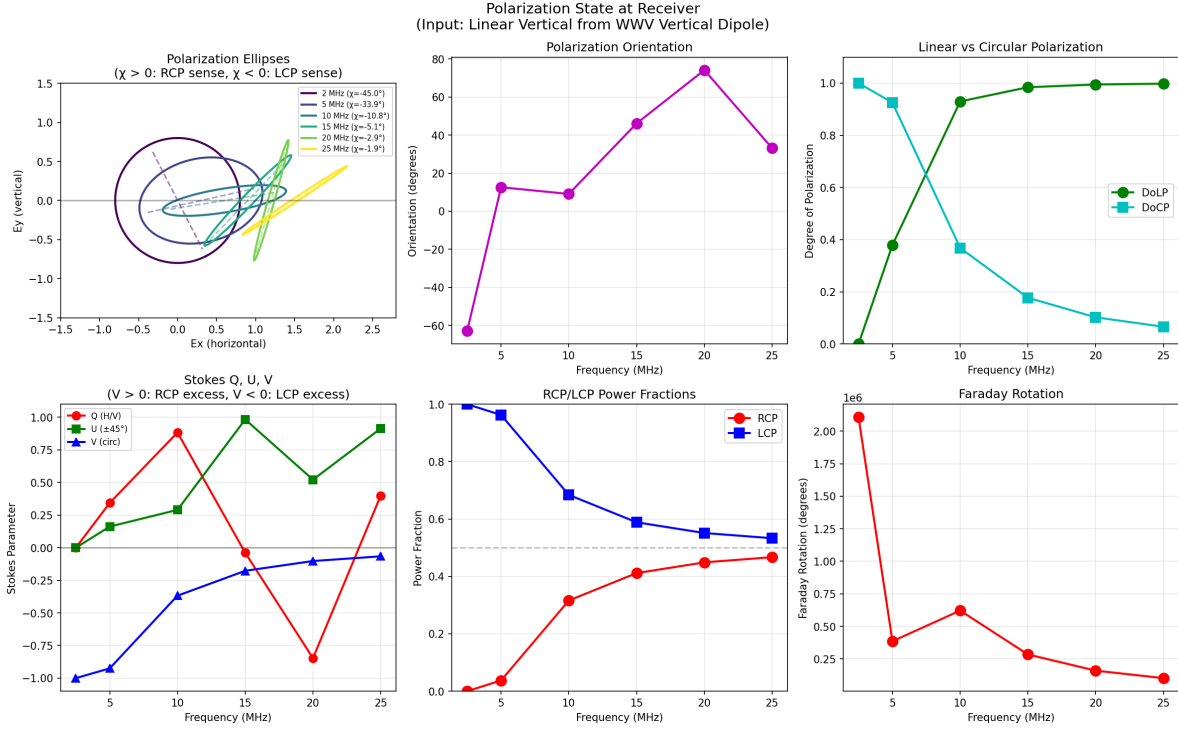


Figure 7: Received polarization state for WWV-to-Boston daytime path. The ellipses at lower frequencies are nearly circular (pure LCP).

10 Three-Dimensional Ray Visualization

The simulator generates 3D visualizations showing the spatial separation of O and X mode ray paths.

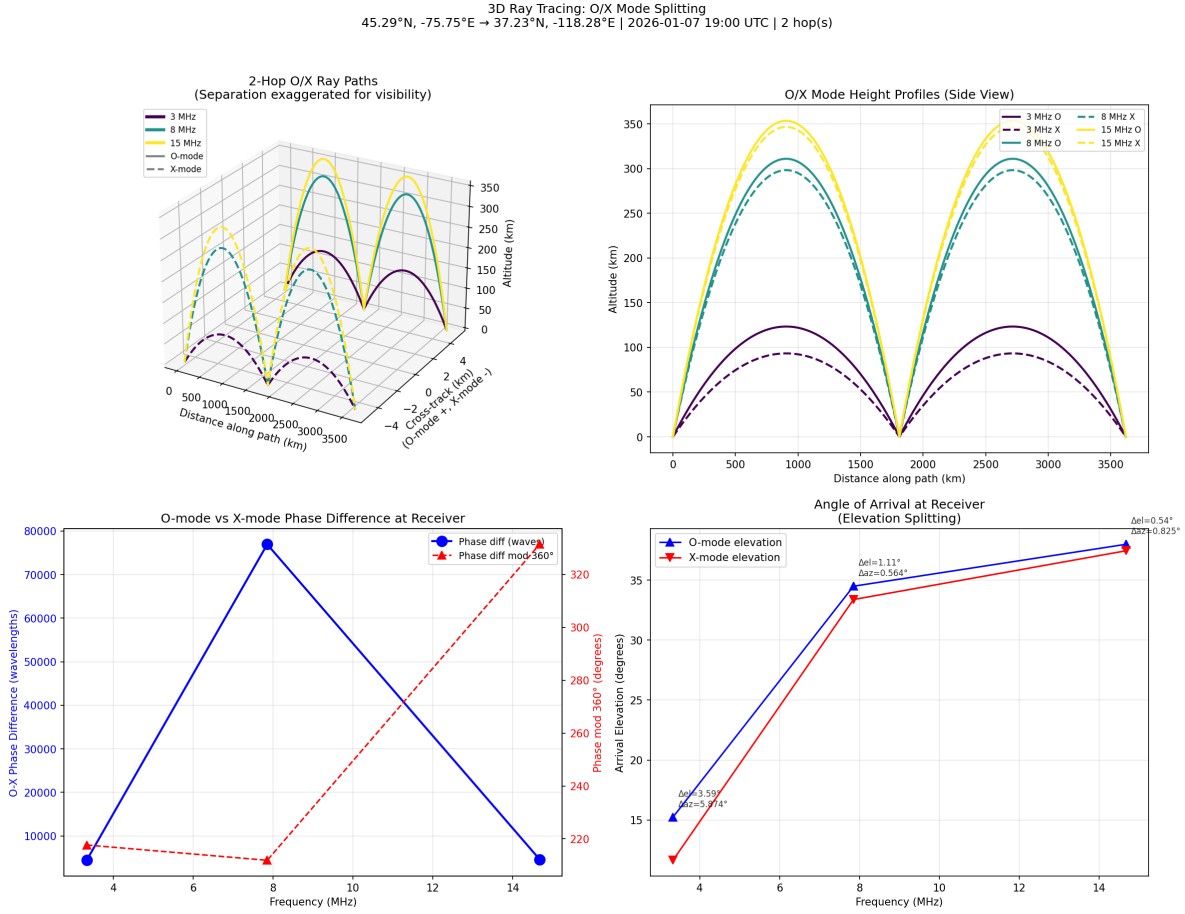


Figure 8: 3D visualization of O and X mode ray paths for CHU-to-OVRO. The O-mode (blue) reflects at higher altitude than X-mode (red), resulting in different arrival angles at the receiver.

11 Observational Evidence

11.1 CHU Triplet Recordings

Simultaneous recordings of CHU signals at 3.33, 5.0, and 7.85 MHz provide observational confirmation of the theoretical predictions. These “triplet” recordings were made using KiwiSDR receivers with circular polarization antennas.

11.1.1 Daytime Observations (2026-01-07, 13:13 UTC)

Conditions: Solar illumination across the propagation path, D-region fully ionized.

Table 6: Daytime triplet analysis results (CHU frequencies)

Frequency (MHz)	Valid Time (%)	RMS @ 20ms (rad)	Fade Fraction (%)	Assessment
3.33	76	0.11	24.1	Good - stable propagation
5.0	70	0.13	29.9	Good - slight degradation
7.85	69	0.13	30.9	Good - near MUF

During daytime, all three frequencies show similar behavior with:

- $\sim 70\%$ valid time (signal above threshold)
- Phase stability (RMS @ 20 ms) of 0.11–0.13 radians ($\sim 7^\circ$)
- Moderate fading ($\sim 25\text{--}30\%$)

The similarity across frequencies during daytime reflects the D-region absorption equalizing propagation conditions—the highly absorbing D-region suppresses multiple modes and paths.

11.1.2 Nighttime Observations (2026-01-07, 00:44 UTC)

Conditions: Path in darkness, D-region largely absent.

Table 7: Nighttime triplet analysis results (CHU frequencies)

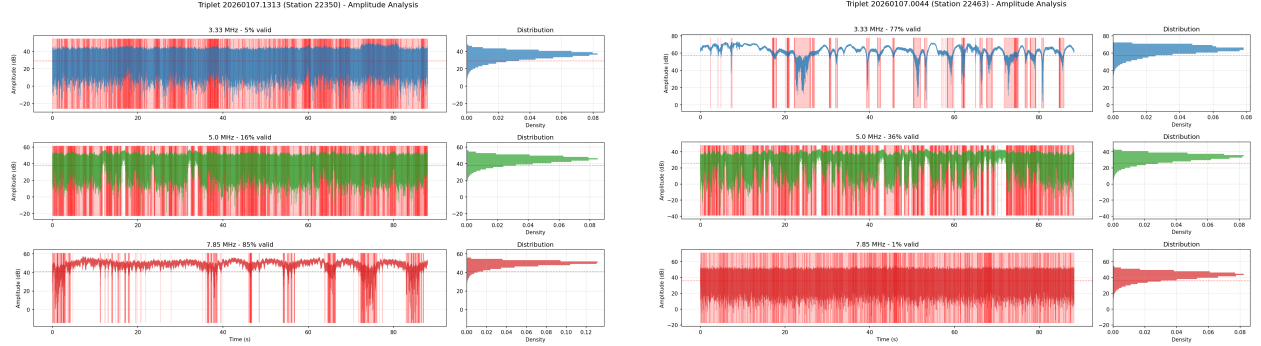
Frequency (MHz)	Valid Time (%)	RMS @ 20ms (rad)	Fade Fraction (%)	Assessment
3.33	77	0.18	23.5	Good - stable
5.0	36	0.57	64.4	Marginal - multipath
7.85	1	5.97	98.5	Poor - above MUF

The nighttime behavior is dramatically different:

- **3.33 MHz:** Good propagation, similar to daytime
- **5.0 MHz:** Severe fading (64%), marginal phase stability
- **7.85 MHz:** Nearly complete fade (98.5% fade time)

This demonstrates the effect of the lower nighttime MUF. At night:

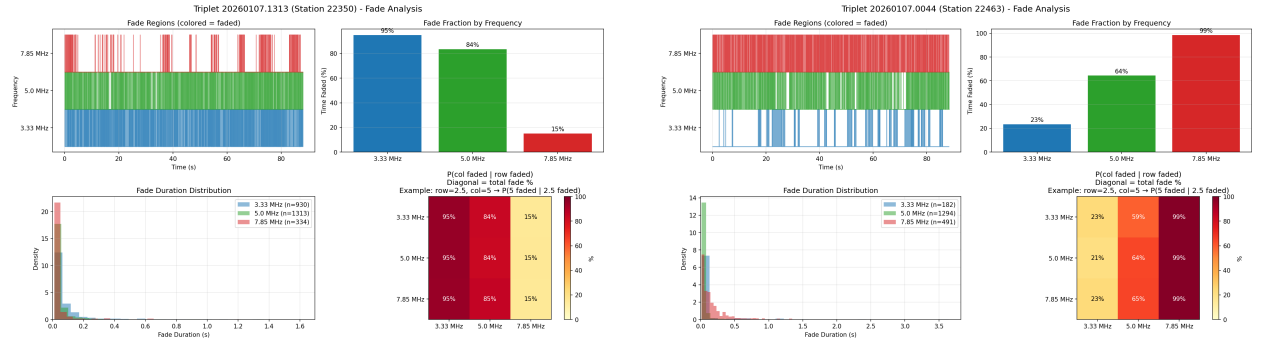
- The F-layer maximum electron density decreases
- The MUF drops from ~ 13 MHz (day) to ~ 5 MHz (night)
- Frequencies above the MUF either penetrate the ionosphere or experience severe multipath
- The absence of D-region absorption allows more multipath propagation at lower frequencies



(a) Daytime: Similar amplitudes across frequencies

(b) Nighttime: Strong frequency dependence

Figure 9: Comparison of triplet amplitude behavior. During daytime (left), all frequencies show similar amplitude variations. At night (right), 7.85 MHz nearly disappears while 3.33 MHz remains stable.



(a) Daytime: Low correlation between frequencies

(b) Nighttime: 7.85 MHz in nearly constant fade

Figure 10: Fade correlation analysis. The conditional probabilities show whether fading at one frequency predicts fading at another.

11.2 Phase Stability: Evidence for Ionospheric Multipath

The phase structure function $D(\tau) = \langle [\phi(t + \tau) - \phi(t)]^2 \rangle$ provides insight into the nature of ionospheric fading.

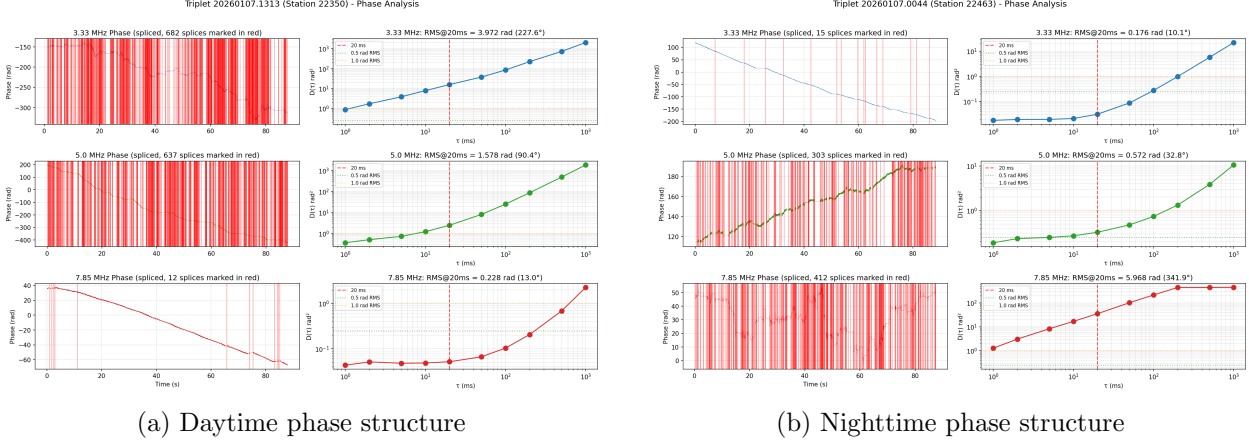


Figure 11: Phase structure functions showing stability vs time lag. The RMS phase at 20 ms lag is a key metric for adaptive correction feasibility.

Key observations from the phase analysis:

- Daytime phase stability is excellent (<0.2 rad RMS at 20 ms)
- Nighttime 5 MHz shows increased phase variance, consistent with multipath
- The 7.85 MHz nighttime signal (when present) shows severe phase instability

11.3 Cross-Frequency Correlation

Analysis of amplitude correlations between frequency pairs reveals:

Daytime:

- Low correlation between frequencies ($r < 0.1$)
- Independent fading at each frequency
- Consistent with frequency-dependent ionospheric scattering

Nighttime:

- Essentially zero correlation ($r \approx 0$)
- Fading at 7.85 MHz is nearly continuous, independent of other frequencies
- Consistent with propagation above MUF

11.4 Comparison with Simulation Predictions

The observations are consistent with simulation predictions:

Table 8: Simulation vs observation comparison

Parameter	Condition	Simulation	Observation
Daytime MUF	19:00 UTC	13 MHz	~10 MHz (7.85 OK)
Nighttime MUF	06:00 UTC	5.2 MHz	~5 MHz (7.85 faded)
Day 3.33 MHz fade	D-region present	Moderate	24%
Night 3.33 MHz fade	D-region absent	Moderate	23%
Night 7.85 MHz fade	Above MUF	Severe	98.5%

The qualitative agreement validates the simulation model. The observation that 7.85 MHz fails at night while 3.33 MHz propagates well confirms the MUF predictions.

12 Implications and Applications

12.1 Time and Frequency Standards

For reception of WWV, CHU, and similar time signals:

- Daytime reception at low frequencies (<10 MHz): LCP antenna essential
- Nighttime reception: Antenna type less critical
- For 24-hour automated systems: Consider switchable or dual-polarization

12.2 Amateur Radio

For HF amateur operations:

- Daytime 80m and 40m bands: Strong LCP advantage
- Higher bands (20m, 15m, 10m): Moderate LCP advantage during day
- Night operations: Polarization less critical

12.3 Direction Finding

For HF DF systems:

- Circular polarization can isolate individual modes
- Reduces bearing errors from O/X mode mixing
- Particularly important for precision applications

12.4 Ionospheric Research

The differential absorption provides a tool for ionospheric studies:

- D-region absorption can be inferred from O/X amplitude ratio
- Faraday rotation measurements give integrated electron content
- Mode separation enables study of individual propagation paths

12.5 Useful HF Beacon Stations

Several time and frequency standard stations provide excellent continuous-wave (CW) sources for ionospheric propagation studies. Their precisely known frequencies, continuous operation, and geographic distribution make them ideal for polarization and fading research.

12.5.1 WWV (Fort Collins, Colorado, USA)

Frequency	Power	Notes
2.5 MHz	2.5 kW	Good for nighttime, high D-region absorption daytime
5.0 MHz	10 kW	Primary low-band frequency
10.0 MHz	10 kW	Good day/night coverage
15.0 MHz	10 kW	Daytime propagation
20.0 MHz	2.5 kW	Daytime, solar maximum
25.0 MHz	Experimental	Intermittent, high solar activity

Location: 40.68°N, 105.04°W (near Fort Collins, Colorado)

Special feature: Since November 2021, WWV broadcasts a HamSCI ionospheric research signal at minute 8 of each hour, consisting of tones, chirps, and noise bursts designed for propagation studies.

12.5.2 WWVH (Kauai, Hawaii, USA)

Frequency	Power
2.5 MHz	5 kW
5.0 MHz	10 kW
10.0 MHz	10 kW
15.0 MHz	10 kW

Location: 21.99°N, 159.76°W (Kauai, Hawaii)

Note: Uses female voice announcements to distinguish from WWV. Useful for transpacific paths. HamSCI research signal at minute 48.

12.5.3 CHU (Ottawa, Canada)

Frequency	Power	Notes
3.330 MHz	3 kW	Good nighttime, avoids WWV interference
7.850 MHz	5 kW	Primary frequency (changed from 7.335 MHz in 2009)
14.670 MHz	3 kW	Daytime propagation

Location: 45.29°N, 75.75°W (Ottawa, Ontario)

Advantage: Frequencies chosen to avoid WWV/WWVH interference, allowing simultaneous monitoring. Lower power but excellent for eastern North American paths.

12.5.4 RWM (Moscow, Russia)

Frequency	Power	Notes
4.996 MHz	5 kW	4 kHz below WWV 5 MHz
9.996 MHz	8 kW	4 kHz below WWV 10 MHz
14.996 MHz	8 kW	4 kHz below WWV 15 MHz

Location: 55.75°N, 37.62°E (Moscow)

Mode: N0N (unmodulated carrier) and A1A (CW). Transmits carrier 0–8 minutes past hour, identifies in Morse at minute 9, 10 Hz pulses minutes 20–30.

Note: Frequencies are deliberately offset from WWV by 4 kHz. Difficult to receive in North America due to WWV interference, but excellent for European and Asian paths. The offset allows simultaneous reception of both stations with sufficient receiver selectivity.

12.5.5 Frequency Coverage Summary

Station	2.5	3.3	5.0	7.9	10	14.7	15	20
WWV	•		•		•		•	•
WWVH	•		•		•		•	
CHU		•		•		•		
RWM			≈		≈		≈	

• = on frequency, ≈ = offset by 4 kHz (RWM at 4.996, 9.996, 14.996 MHz)

12.5.6 Practical Considerations for Ionospheric Research

- **Frequency triplets:** CHU's three frequencies (3.33, 7.85, 14.67 MHz) span a 4.4:1 range, ideal for studying frequency-dependent ionospheric effects
- **WWV coverage:** Six frequencies from 2.5–25 MHz provide comprehensive band coverage
- **Geographic diversity:** WWV (Colorado), WWVH (Hawaii), CHU (Ottawa), RWM (Moscow) enable multi-path studies
- **Continuous operation:** All stations broadcast 24/7, enabling long-term monitoring
- **Phase coherence:** All transmissions are referenced to atomic standards, enabling precise phase measurements
- **600 Hz modulation:** WWV and CHU include 600 Hz tone modulation, useful for measuring ionospheric dispersion across ±600 Hz bandwidth

13 Conclusions

1. **Differential absorption is real and significant:** X-mode (RCP in Northern Hemisphere) suffers substantially more D-region absorption than O-mode (LCP). The difference can exceed 60 dB at lower frequencies during daytime.

2. **Received polarization is often strongly elliptical:** During daytime at frequencies below 10 MHz, the received signal can be nearly pure circular polarization due to elimination of one mode.
3. **Handedness matters enormously:** For daytime HF reception in the Northern Hemisphere, LCP antennas provide dramatic SNR advantages over RCP—sometimes the difference between signal and no signal.
4. **Circular polarization eliminates Faraday fading:** But it does NOT eliminate multipath fading from ionospheric irregularities, which is the dominant residual fading mechanism.
5. **Dual-polarization receivers offer diversity gain:** Because O and X modes follow paths separated by 15–40 km, their multipath fading is partially decorrelated. Dual-polarization (LCP+RCP) receivers can exploit this for diversity combining, potentially providing 5–10 dB improvement even when mode powers are comparable.
6. **The effect is frequency and time dependent:** Strongest at low frequencies, during daytime, on longer paths. Negligible at night when the D-region disappears.
7. **Practical antenna selection should consider these effects:** For serious HF work, especially at lower frequencies, circular polarization antenna selection is not optional—it's essential for optimal performance. Dual-polarization systems provide benefits in all conditions.

A Simulation Code

The simulations in this report were generated using the `multihop_3d.py` Python script, which implements:

- Full 3D ray tracing with O/X mode separation
- Appleton-Hartree refractive index calculation
- D-region absorption with differential O/X coefficients
- Faraday rotation integration along ray path
- Stokes parameter calculation for received polarization

Example usage:

```
python3 multihop_3d.py \
--tx-lat 45.2917 --tx-lon -75.7533 \
--rx-lat 37.23 --rx-lon -118.28 \
--frequencies 3.33 7.85 14.67 \
--hops 2 \
--output chu_ovro_day \
--date "2026-01-07T19:00:00"
```

B Stokes Parameter Definitions

The Stokes parameters (I, Q, U, V) fully characterize the polarization state:

$$I = |E_x|^2 + |E_y|^2 \quad (\text{total intensity}) \quad (26)$$

$$Q = |E_x|^2 - |E_y|^2 \quad (\text{linear horizontal/vertical}) \quad (27)$$

$$U = 2 \operatorname{Re}(E_x E_y^*) \quad (\text{linear } \pm 45^\circ) \quad (28)$$

$$V = 2 \operatorname{Im}(E_x E_y^*) \quad (\text{circular: } + = \text{RCP}, - = \text{LCP}) \quad (29)$$

For fully polarized radiation: $I^2 = Q^2 + U^2 + V^2$

Derived quantities:

$$\text{Degree of linear polarization} = \frac{\sqrt{Q^2 + U^2}}{I} \quad (30)$$

$$\text{Degree of circular polarization} = \frac{|V|}{I} \quad (31)$$

$$\text{Orientation angle} = \frac{1}{2} \arctan \left(\frac{U}{Q} \right) \quad (32)$$

$$\text{Ellipticity angle } \chi = \frac{1}{2} \arcsin \left(\frac{V}{I} \right) \quad (33)$$